The Electron Transfer System of Syntrophically Grown *Desulfovibrio vulgaris*

Christopher B. Walker[1,8,§], Zhili He[2,3,8], Zamin K. Yang[2,8], Joseph A. Ringbauer, Jr. [4,8], Qiang He[2,8], Jizhong Zhou[2,3,8], Gerrit Voordouw[5], Judy D. Wall[4,8], Adam P. Arkin[6,7,8], Terry C. Hazen[7,8], Sergey Stolyar[1,8] and David A. Stahl[1,8,*]

[1]Department of Civil and Environmental Engineering, University of Washington
[2]Biosciences Division, Oak Ridge National Laboratory
[3]Institute For Environmental Genomics and Department of Botany and Microbiology, University of Oklahoma
[4]Biochemistry Division and Molecular Microbiology and Immunology Department, University of Missouri
[5]Department of Biological Sciences, University of Calgary
[6]Department of Bioengineering, University of California, Berkeley
[7]Earth Sciences Division, Lawrence Berkeley National Laboratory
[8]Virtual Institute for Microbial Stress and Survival (vimss.lbl.gov)

* Corresponding author:
Dr. David A. Stahl
Department of Civil and Environmental Engineering
University of Washington
302 More Hall, Box 352700
Seattle, WA 98195-2700, USA.
Phone: (206) 685-3464
Fax: (206) 685-9185
E-mail: dastahl@u.washington.edu

§ Present address:
Geosyntec Consultants
1370 Stewart Avenue, Suite 205
Seattle, WA 98104

Figures: 3
Tables: 2

Running Title: SRM Syntrophic Metabolism

ABSTRACT

Interspecies hydrogen transfer between organisms producing and consuming hydrogen promotes the decomposition of organic matter in most anoxic environments. Although syntrophic couplings between hydrogen producers and consumers are a major feature of the carbon cycle, mechanisms for energy recovery at the extremely low free energies of reactions typical of these anaerobic communities have not been established. In this study, comparative transcriptional analysis of a model sulfate-reducing microbe, *Desulfovibrio vulgaris* Hildenborough, suggested the use of alternative electron transfer systems dependent upon growth modality. During syntrophic growth on lactate with a hydrogenotrophic methanogen, *D. vulgaris* up-regulated numerous genes involved in electron transfer and energy generation when compared with sulfate-limited monocultures. In particular, genes coding for the putative membrane-bound Coo hydrogenase, two periplasmic hydrogenases (Hyd and Hyn) and the well-characterized high-molecular weight cytochrome (Hmc) were among the most highly expressed and up-regulated. Additionally, a predicted operon coding for genes involved in lactate transport and oxidation exhibited up-regulation, further suggesting an alternative pathway for electrons derived from lactate oxidation during syntrophic growth. Mutations in a subset of genes coding for Coo, Hmc, Hyd and Hyn impaired or severely limited syntrophic growth but had little affect on growth via sulfate-respiration. These results demonstrate that syntrophic growth and sulfate-respiration use largely independent energy generation pathways and imply that understanding of microbial processes sustaining nutrient cycling must consider lifestyles not captured in pure culture.

INTRODUCTION

Nutrient cycling on earth is determined primarily by cooperative interactions among microorganisms. The sharing of available energy within communities is particularly important in anaerobic systems, where limited energy is divided among highly specialized and metabolically interdependent populations (36, 37, 39). In the absence of exogenous electron acceptors such as sulfate and nitrate, the mineralization of organic matter in anoxic environments yields primarily carbon dioxide and methane - a process controlled by the synergistic activities of multiple anaerobic microbial populations. To better understand the metabolic basis and ecological significance of these syntrophic associations, we constructed an archetypical "community of two" by pairing *Desulfovibrio vulgaris* Hildenborough with a hydrogenotrophic methanogen, *Methanococcus maripaludis* strain S2.

D. vulgaris is a representative of sulfate-reducing microorganism, coupling the oxidation of characteristic substrates such as H_2, lactate or ethanol with the reduction of sulfate to sulfide (for review see (32). In the absence of sulfate, *D. vulgaris* (and SRM in general) ferment organic acids and alcohols, producing hydrogen, acetate and carbon dioxide by forming syntrophic associations with hydrogen consuming populations (3, 23, 40). These alternative lifestyles might be sustained by distinct metabolic systems, possibly reflected in part by the large number of hydrogenases and electron transfer complexes described in past biochemical studies and more recently revealed in the *D. vulgaris* Hildenborough genome sequence (14, 32). Thus, even though sulfate-respiration and syntrophic growth both produce the same oxidized end products (acetate and carbon dioxide), mechanistic differences in electron transfer pathways likely exist. These differences were evaluated by comparing whole-genome transcriptional profiles of *D. vulgaris* Hildenborough grown

continuously on lactate under two culture conditions: syntrophic cocultures (lacking sulfate) and sulfate-limited monocultures. Complementary mutant studies showed that among genes highly up-regulated during syntrophic growth, at least two (coding for the Coo hydrogenase and the high-molecular weight cytochrome complex) were required for efficient syntrophic growth but not for sulfate respiration.

MATERIALS AND METHODS

Strains

Transcriptional analyses were performed using *Desulfovibrio vulgaris* Hildenborough and *Methanococcus maripaludis* S2. Additionally, four mutant strains (3 described in previous investigations and 1 described here) of *D. vulgaris* were used during phenotypic growth comparisons. Details of all six strains are provided in Table 1.

Biomass production

Three biological replicates of cocultures and sulfate-limited *D. vulgaris* monocultures were grown in a chemostat in coculture medium (CCM) containing 30 mM sodium DL-lactate (coculture and monoculture) and 10 mM Na_2SO_4 (monoculture only). CCM also contained a basal salt solution consisting of the following components per liter: 2.17 g NaCl, 5.5 g $MgCl_2 \cdot 6H_2O$, 0.14 g $CaCl_2 \cdot 2H_2O$, 0.5 g NH_4Cl and 0.335 g KCl. The medium was buffered using 1.1 mM of K_2HPO_4 and 30 mM $NaHCO_3$ with 1 ml of nonchelated trace elements (46) and 1 ml of vitamin solution amended with 2.0 g/l choline chloride (2) added as growth supplements. L-cysteine•HCl (1 mM) and sulfide (1 mM $Na_2S \cdot 9H_2O$) were added as reducing agents. Resazurin (1 mg/L) was added as a redox indicator. Stock solutions of K_2HPO_4 (1 M), $NaHCO_3$ (6.0 M), L-cysteine•HCl (1 M), $Na_2S \cdot 9H_2O$ (1 M) and the nonchelated trace elements and vitamin mixtures were

prepared under anoxic conditions. Medium was made by adding salts, sodium DL-lactate, resazurin and Na_2SO_4 (if applicable) to water, then autoclaving. After sterilization, the chemostat or medium reservoir bottle was connected to N_2:CO_2 (90:10) and allowed to cool to room temperature before adding the remaining components.

A 1 ml glycerol stock of previously grown coculture or monoculture was used to inoculate 100 ml of CCM (amended with sulfate for monocultures) in a 200 ml serum vial. Cultures were incubated in the dark at 37 ºC with a shaking speed of 250 rpm. When the cultures reached an $O.D._{600}$ of 0.27 ± 0.01, they were transferred to a 3 L FairMenTec chemostat (Wald, Switzerland) filled with 2 L of CCM (amended with sulfate for monocultures). Following inoculation, the chemostat was run in batch mode at 37ºC with a stirring speed of 250 rpm. The pH was maintained at 7.0 – 7.2 via bicarbonate buffer and small automated additions of 0.1 M NaOH or HCl as needed. A blanket of N_2:CO_2 (90:10) gas mixture was flushed through a sterile cotton plug before entering the headspace of the reactor, with the flow rate maintained at 0.20 ml/min using an Alicat Scientific mass controller (MC-20SCCM-D, Tucson, AZ). Headspace concentrations of CH_4, CO_2, H_2, H_2S, O_2 and N_2 were monitored at 30 min intervals using a Hiden Analytical QIC-20 mass spectrometer (Warrington, U.K.). Lactate, acetate, ethanol, glycerol and formate were measured enzymatically as previously described (40). Continuous culture operation was initiated after absorbance measurements reached approximately 0.27 (OD_{600}). A dilution rate of 0.039 h^{-1} was maintained and biomass harvested when the variance of $O.D._{600}$ readings was less than 10% over a period of three retention periods. Samples were taken regularly for direct cell counts and protein measurements. *Desulfovibrio*:*Methanococcus* cell ratios were determined through DAPI-stained cell counts. Total protein measurements were

determined using the Coomassie Plus Assay (Pierce, Rockford, IL). Cells were harvested using an ice-chilled sterile stainless steel tube connected to the chemostat medium exhaust line. Culture fluid was transferred to Falcon tubes (50 ml) that had been stored in an anoxic chamber and pre-chilled on ice. The tubes were centrifuged for 15 min at 3,220 x *g* at 4ºC. After centrifugation, the supernatant was poured off and tubes immediately frozen at –80 ºC.

Transcriptional analysis

Whole genome microarrays containing 3,482 of the 3,531 protein-coding sequences for *D. vulgaris* Hildenborough were synthesized as previously described (4) onto UltraGAPS glass slides (Corning Life Sciences, Corning, NY) using a BioRobotics Microgrid II microarrayer (Genomic Solutions, Ann Arbor, MI). Each slide contained duplicate spots for each protein-coding sequence and each biological replicate was hybridized to at least three slides. Thus each $\log_2$ expression level described within this study were obtained from triplicate biological replicates, each with at least six technical replicates (duplicate on-chip technical replicates and at least three microarray slide replicates).

RNA isolation, quantification and transcription were performed as previously described (4). Briefly, total cellular RNA was isolated using TRIzol reagent (Invitrogen, Carlsbad, CA), purified using the RNeasy Mini kit (Qiagen, Valencia, CA) with on-column DNase digestion using an RNase-free DNase set (Qiagen, Valencia, CA). The cDNA probes were generated from 10 µg of purified total RNA using reverse transcriptase and then labeled (43). Random hexamers (Invitrogen, Carlsbad, CA) were used for priming and the fluorophone Cy5-dUT (Amersham Biosciences, Piscataway, NJ) was used for labeling. After labeling, RNA was removed by NaOH treatment and cDNA immediately

purified using a Qiagen PCR Mini kit. Genomic DNA was extracted from cell pellets using the Qbiogene FastDNA SPIN Kit for Soil (Mp Biomedicals, Solon, OH). Extracted gDNA was labeled with the fluorophone Cy3-dUTP (Amersham Biosciences, Piscataway, NJ). Labeling efficiencies were routinely monitored by measuring absorbances at 260 nm (for DNA concentrations), 550 nm (for Cy3) or 650 nm (for Cy5).

Cy3-dUTP-labeled genomic DNA for *D. vulgaris* was aliquoted for triplicate arrays and co-hybridized with Cy5 labeled cDNA (41, 47). Co-hybridization using dried probes mixed and resuspended in 35-40 µl of hybridization solution containing 50% (v/v) formamide, 5x saline-sodium citrate (SSC; 1x SSC is 0.15 M NaCl, 0.015 M sodium citrate, pH 7.0), 0.1% (w/v) sodium dodecyl sulfate (SDS) and 0.1 mg/ml herring sperm DNA (Invitrogen, Carlsbad, CA). The hybridization solution was incubated at 95 to 98ºC for 5 min, centrifuged briefly, incubated at 50ºC and applied onto microarray slides. Hybridization was carried out in hybridization chambers (Corning Life Sciences, Corning, NY) at 45ºC overnight (16-20 h). At each end of the microarray slide, 10 µl of 3x SSC solution was added to maintain proper humidity and probe hydration. Slides were washed twice in a solution containing 2x SSC and 0.1% (w/v) SDS at 42ºC for 5 min, twice in a solution containing 0.1x SSC and 0.1% (w/v) SDS at room temperature for 10 min and twice in 0.1x SSC at room temperature for 1 min. After drying under a stream of N_2, the slides were scanned for Cy5 and Cy3 fluorophores using the ScanArray Express microarray analysis system (Perkin Elmner, Waltham, MA). Fluorescence intensities for each spot were determined using 16-bit TIFF scanned images and quantified with ImaGene software (v 6.0, Biodiscovery, Marina Del Rey, CA). Any spot with fewer than 75% of pixels or more than 3 standard deviations above the local background in both channels was rejected (10).

For each array, signal intensities, spot quality and background intensities of each spot were quantified with ImaGene software (v 6.0, Biodiscovery, Marina Del Rey, CA). Computational analyses to determine the expression ratios, log ratios, Z scores, as well operon-based estimates of local accuracy were done as previously described (4, 25). Briefly, the $\log_2$ expression was normalized globally by calculating the net signal for each spot. This was done by subtracting the background and adding a pseudosignal of 100, thereby enforcing a positive value. If the resulting net signal was less than 50, a value of 550 was used. Following this, the expression levels for each spot were calculated from the ratio of the mRNA over gDNA (Cy3 channel over Cy5 channel). Expression levels for each replicate were normalized such that the total expression over the present spots was identical. Mean expression levels and standard deviations of each spot were estimated, requiring $n > 1$, where n is the number of scorable replicates. To estimate the differential gene expression between the control and treatment conditions, normalized log ratios were calculated. Each log ratio was calculated as $\log_2$(coculture) – $\log_2$(monoculture). This log ratio was normalized using locally weighted scatterplot smoothing (LOWESS) on the difference versus the sum of the log expression level (7). Since sector-based artifacts were detected, each log ratio was further normalized by subtracting the median of all spots within each sector. The final normalized log ratio ($\log_2$R) was calculated from the average ratio of spots for each gene. The significance of the normalized log ratio was assessed using a Z score calculated as follows (where 0.25 is a pseudovariance term):

$$Z = \frac{\log_2(\text{coculture/monoculture})}{\sqrt{0.25 + \sum \text{variance}}}$$

Z scores were determined using operon-based estimates of local accuracy as a guide, where each point represents a group of 100 predicted significant changers with similar Z

scores. The estimated accuracy of each changer group was derived by inspecting other genes in the same operon as these changers. For random changers, the transcripts for 50% of these genes should have been regulated in the same direction, while for perfect changers 100% of the genes should have been regulated in the same direction. Members of the operons without a consistent signal across replicates ($Z < 0.25$) were excluded. The operon-based estimates of local accuracy calculated for this experiment suggested absolute values of Z scores greater than 1.0 signified statistically significant up- or down-regulation (Supplemental Figure 1).

Mutant construction

The generation of the *hmc*, *hyd*, and *hyn* deletion mutants have been previously described (6, 11, 31). The *cooL* transposon mutant was generated by conjugation between *D. vulgaris* and *E. coli* BW20767 (pRL27) (19). The conjugation protocol was a modified method of Fu and Voordouw (9). Briefly, cultures of *D. vulgaris* were grown to mid-exponential phase, and combined in a 3:1 or 6:1 ratio with the *E. coli* donor grown to early exponential phase in LC medium (1.0% [wt/vol] tryptone, 0.5% [wt/vol] yeast extract, and 0.5% [wt/vol] NaCl). Mating mixtures were concentrated by centrifugation. The concentrated cells were placed onto filter discs (0.22 μm pore diameter, GSWP, Millipore Billerica, MA), the discs placed on the surface of solidified LS4 (LS4D with 1% [wt/vol] yeast extract added), and incubated for sixteen hours at 34°C (25). The cells were then washed from the membrane with 2 ml LS4 medium. After six hours of incubation, antibiotic G418 (400 μg/ml) was added to select for the transposon mutants and nalidixic acid (200 μg/ml) was added to select against the *E. coli* donor. Cells were then spread onto LS4 agar (100 - 500 μl/plate) containing both antibiotics and incubated in an anaerobic growth chamber at 34°C for at least four days for colony growth.

The chromosomal localization of the transposon insertions was identified by sequencing DNA after semi-random PCR amplification using a variation of a previously described protocol (5). One microliter of a 50-µl boiled single-colony suspension in distilled H_2O was used as the template DNA in a 20-µl PCR mixture containing primer tpnRL17-1 (5'-AAC AAG CCA GGG ATG TAA CG-3') and either primer CEKG 2A (5'-GGC CAC GCG TCG ACT AGT $AC(N)_{10}$ AGA G-3'), CEKG 2B (5'-GGC CAC GCG TCG ACT AGT $AC(N)_{10}$ ACG CC-3') or CEKG 2C (5'-GGC CAC GCG TCG ACT AGT $AC(N)_{10}$ GAT AT-3'). One microliter of a 1:5 dilution of this reaction mixture was used as the template DNA for a second PCR performed with primers tpnRL17-2 (5'-AGC CCT TAG AGC CTC TCA AAG CAA-3') and CEKG 4 (5'-GGC CAC GCG TCG ACT AGT AC-3'). Thermocycler conditions were as previously described (5). Samples that produced distinct PCR products on an agarose gel after the second reaction were cleaned with a PCR purification kit (Qiagen,Valencia, CA) and sequenced by using primer tpnRL17-1. The chromosomal locations of the insertions were identified by BLAST analysis of the sequences adjacent to the transposon.

Phenotypic growth analyses

All phenotypic growth assays were carried out in 17 ml Hungate tubes equipped with rubber stoppers and screw-tops. Cultures were incubated at 37 ºC in the dark with a 300 rpm shaking speed. Each tube contained 8 ml of CCM amended with 30 mM of electron donor (lactate or pyruvate) and 30 mM of sulfate (if applicable). The headspace contained an overpressure of 180 mbar of N_2:CO_2 (80:20). Dilution series out to 10^{-8} were initiated from 1 ml glycerol stocks of each *Desulfovibrio* mutant and *Methanococcus*. *Desulfovibrio* cultures were grown in CCM amended with 30 mM

sulfate. *Methanococcus* cultures were grown in CCM lacking lactate and amended with 5 mM acetate and 250 mbar overpressure of H_2:CO_2 (80:20). Cocultures were established by combining 1 ml of exponentially growing *Desulfovibrio* and 0.5 ml of exponentially growing *Methanococcus* from the highest dilutions. Cocultures were transferred (1% v/v) three times to ensure dilution of any residual sulfate/acetate or H_2 before inoculating triplicate tubes for growth experiments. Tubes were monitored for growth using $O.D._{600}$ readings blanked against uninoculated medium. Biomass concentrations were estimated using the previously published conversion values of 1.0 $O.D._{600}$ = 0.385 g dry coculture biomass/L (40) and 1.0 $O.D._{600}$ = 0.309 g dry monoculture biomass/L (45). Growth yields were estimated using the maximum $O.D._{600}$ value, which corresponded with complete consumption of the 30 mM electron donor present. Errors represent the standard deviation of triplicate samples. Lactate-to-pyruvate, $lactate_{coculture}$-to-$lactate_{monoculture}$ and $pyruvate_{monoculture}$-to-$pyruvate_{monoculture}$ growth yield ratios were calculated using these estimated yields. The estimated yields and ratios were compared with previously published values of *D. vulgaris* grown in monoculture and in coculture with *Methanosarcina barkeri* (44).

RESULTS

Continuous cultures of syntrophically grown *D. vulgaris* and *M. maripaludis* on 30 mM lactate (without sulfate) were maintained using a dilution rate of 0.039 hr^{-1} (Figure 1). Steady-state concentrations of lactate ranged from 3 – 5 mM during continuous operation, indicating nearly complete utilization of the 30 mM addition. Acetate (24-27 mM) was the principal by-product produced, although small quantities of ethanol (0.02-0.1 mM) were detected throughout batch and continuous culture. Glycerol and formate, other potential by-product of lactate fermentation, were not detected at the 0.1 mM limit

of detection. Methane production began within 12 hours of inoculation and remained relatively stable during steady-state growth, although some fluctuations were routinely observed. These fluctuations occurred immediately after initiation of continuous culture operations and were likely a result of pressure differentials contained in the sampling inlet, not biological variation. The gas concentration values displayed in Figure 1 are lower than the predicted stoichiometry of lactate oxidation, reflecting loss as dissolved methane in the liquid effluent and in the headspace by N_2/CO_2 gas flow during operation of the reactor. The methane values primarily served to assess steady-state operation. A *Desulfovibrio*-to-*Methanococcus* cell ratio of 4:1 was maintained during steady-state growth.

Whole-genome transcriptional analysis revealed highly divergent profiles between *Desulfovibrio* growing in coculture versus sulfate-limited monoculture (Supplemental Tables 1 and 2). Syntrophically grown *D. vulgaris* up-regulated 169 open-reading frames (ORFs) and down-regulated 254 ORFs compared with sulfate-limited monocultures grown at the same generation time. ORFs were considered to have statistically significant up- or down-regulation if the absolute value of the Z-score was greater than 1.0 , as determined through operon-based estimates of local accuracy (Supplemental Figure 1). Clustering into orthologous groups (COGs) showed that those associated with energy production and conservation were the most highly up-regulated, both by proportion and number (20% and 42 respectively, see Supplemental Figure 2). The largest number of down-regulated genes were in the signal transduction group (46 out of 273) and inorganic ion transport and metabolism (23 out of 105). Every COG exhibited at least one statistically significant changer, based on an absolute Z-score of greater than one.

Among the largest expression increases were in operons coding for three multisubunit transmembrane proteins associated with electron transfer reactions: the high-molecular weight cytochrome (Hmc, DVU0531-6), a cytoplasmic hydrogenase (Coo, DVU2286 – 93, $\log_2R$ = 1.1-1.7), and a putative heterodisulfide reductase (Hdr, DVU2399-405, $\log_2R$ = 1.0-1.6). Significant increases in expression were also observed for genes coding for a transmembrane three-subunit molybdopterin-oxidoreductase (DVU0692-4; $\log_2R$ = 1.0), two periplasmic hydrogenases (*hydAB*, DVU1769-70 and *hynAB-1*, DVU1921-2; $\log_2R$ = 1.0-2.0), an alcohol dehydrogenase (Adh, DVU2405, $\log_2R$ = 3.0), and an aldehyde-ferredoxin oxidoreductase (Aor, DVU1179; $\log_2R$ = 1.9). Only two genes known to be associated with electron transfer reactions were significantly down-regulated, a flavodoxin gene (DVU2680, $\log_2R$ = -5.2) and an adjacent hypothetical gene (DVU2681).

Syntrophy was also associated with changes in the transcription of genes in a predicted operon (DVU3024-DVU3033) coding for lactate uptake and oxidation. The enzymes in this pathway are predicted to produce acetate, CO_2, ATP, and reduced electron carriers (lactate permease, DVU3026; a putative lactate dehydrogenase related to the membrane-bound glycolate oxidase of *E. coli*, DVU3027-3028; a monomeric pyruvate:ferredoxin oxidoreductase, DVU3025; phosphate acetyltransferase, DVU3029; acetate kinase, DVU3030). The lactate permease and pyruvate oxidase in this operon-like arrangement were clearly up-regulated ($\log_2R$ =1.2 and 2.0, respectively) during syntrophic growth, as was a second lactate permease (DVU2285, $\log_2R$ = 1.4) located up-stream and directly adjacent to the gene for the Coo hydrogenase. The genes coding for the lactate permease (DVU3026) and contiguous lactate dehydrogenase (DVU3027-3028) are conserved in

another lactate-oxidizing syntroph (*Pelomaculum thermopropionicum*) in an operon-like arrangement of the same gene order as in *D. vulgaris* Hildenborough (18).

Despite trace concentrations of sulfate in the growth medium, key genes of sulfate respiration (ATP sulfurylase, adenylyl-sulfate reductase, dissimilatory sulfite reductase, pyrophosphatase, and thiosulfate reductase) were also up-regulated during syntrophic growth, consistent with previous observations of constitutive expression (13, 49). However, none of the sulfate permeases were up-regulated and one (DVU0053) was significantly down-regulated.

Although most differentially expressed genes (ca. 400) have no assigned function (lipoproteins, hypotheticals and conserved hypotheticals), some of the more highly up-regulated have homologs (possible orthologs) in the genomes of characterized bacterial syntrophs. For example, comparative analysis of one up-regulated hypothetical gene cluster (DVU2648-55) found no informative BLAST matches except for DVU2655 encoding a putative D-alanyl-D-alanine carboxypeptidase (*dacA*). The *D. vulgaris* DacA shares highest similarity to proteins in *Syntrophobacter fumaroxidans* and *Syntrophus aciditrophicus* (1). Another cluster of up-regulated and highly expressed ORFs of unknown function (DVU0144-50) share high similarity to genes found in *S. fumaroxidans* (SFUM0625-9).

Complementary analyses of *D. vulgaris* mutants with deletions or disruptions in the *coo*, *hmc*, *hyd* and *hyn* operons (all up-regulated during growth in coculture) provided direct evidence for function in syntrophy. These mutants affected almost exclusively the capacity for syntrophic growth, either greatly inhibiting (Δ*cooL* and Δ*hmc*) or slowing

and slightly inhibiting (Δ*hyd* and Δ*hyn-1*) growth in coculture (Figure 2, Table 2). Notably, among these mutants, only the Δ*hmc* strain showed slightly impaired respiratory growth (approximately 60% maximum cell density when compared with wildtype). The Δ*cooL* and Δ*hmc* mutants were capable of only sparse growth in coculture on lactate, with a maximum cell density approximately 10% of the wildtype. However, when grown in coculture on pyruvate, only the Δ*hmc* mutant was impaired (< 15% maximum cell density of wildtype). Cocultures established with the Δ*hyd* and Δ*hyn-1* mutants achieved cell densities comparable to the wildtype on both lactate and pyruvate but at reduced growth rates. Recovery of *Methanococcus* from all cocultures through addition of H_2 and acetate demonstrated an active hydrogenotrophic population, confirming attribution of the observed growth defects to mutations in *Desulfovibrio*.

DISCUSSION

A conceptual model for electron transfer during syntrophic growth that captures the transcription and mutant data is shown in Figure 3, providing a framework for the following discussion of the electron transfer reactions and energetics of syntrophic growth. Lactate is transported from the periplasm via a dedicated lactate permease (DVU3026) and oxidized to pyruvate by a putative lactate dehydrogenase (DVU3027-8), likely functions primarily during syntrophic growth. The extracted electrons reduce an unknown electron carrier and are shuttled to the Coo hydrogenase, subsequently forming H_2 while concomitantly translocating protons (or sodium) across the cytoplasmic membrane. Pyruvate is oxidized by the pyruvate-oxidoreductase, generating reduced ferredoxin. The membrane associated Hmc complex then couples the oxidation of reduced ferredoxin to the reduction of a periplasmic cytochrome and/or hydrogenases (Hyn-1 and Hyd), yielding hydrogen as a final product.

The standard free energy yields for syntrophic growth on either lactate or pyruvate are well above the generally accepted minimum energy needed to support the two populations (36), but lower for growth on lactate than pyruvate (Equations 4 and 5).

Lactate fermentation:	$C_3H_5O_3^- + H_2O \rightarrow C_2H_3O_2^- + 2\,H_2 + CO_2$	$\Delta G^{o\prime} =$ -8.8 kJ/mol	(1)
Pyruvate fermentation:	$C_3H_3O_3^- + H_2O \rightarrow C_2H_3O_2^- + H_2 + CO_2$	$\Delta G^{o\prime} =$ -52.0 kJ/mol	(2)
Methanogenesis:	$4\,H_2 + CO_2 \rightarrow CH_4 + 2\,H_2O$	$\Delta G^{o\prime} =$ -130.7 kJ/mol	(3)
$Syntrophy_{Lactate}$:	$C_3H_5O_3^- \rightarrow C_2H_3O_2^- + 0.5\,CH_4 + 0.5\,CO_2$	$\Delta G^{o\prime} =$ -74.2 kJ/mol	(4)
$Syntrophy_{Pyruvate}$:	$C_3H_3O_3^- + 0.5\,H_2O \rightarrow C_2H_3O_2^- + 0.25\,CH_4 + 0.75\,CO_2$	$\Delta G^{o\prime} =$ -84.7 kJ/mol	(5)

Using the concentrations observed during steady-state ([lactate] = 4 mM, [acetate] = 26 mM, $[H_2] = 2.5*10^{-5}$ atm, $[CO_2] = 0.05$ atm, $[CH_4] = 0.0006$ atm, T = 310 K) the free energy yields for lactate fermentation (-67.3 kJ/mol, Equation 1) and syntrophic growth on lactate (-82.8 kJ/mol, Equation 4) become more favorable. The lower free energy available for growth on lactate (Equation 4) is determined primarily by the energy cost of the two-electron oxidation of lactate to pyruvate and hydrogen (Equation 8).

Lactate dehydrogenase	$C_3H_5O_3^- + EC_{ox} \rightarrow C_2H_3O_2^- + 2H^+ + EC_{red}$	$\Delta G^{o\prime}$ NA	(6)
Coo Hydrogenase	$EC_{red} + 2H^+ \rightarrow H_2 + EC_{ox}$	$\Delta G^{o\prime}$ NA	(7)
Combined reactions	$C_3H_5O_3^- \rightarrow C_3H_3O_3^- + H_2$	$\Delta G^{o\prime} =$ +43.2 kJ/mol	(8)

Reverse electron flow is thought necessary to sustain lactate oxidation to pyruvate during respiratory growth (42). This cost is also reflected by the lower biomass yield on lactate versus pyruvate for either growth modality (Table 2), as previously observed for *D. vulgaris* Hildenborough paired with a different methanogen (44). Since syntrophic growth on lactate provides considerably less energy than is available through respiration,

we anticipated mechanistic differences in electron transfer reactions governing the initial two-electron oxidation of lactate.

These mechanistic differences were further suggested by the global up-regulation of genes associated with energy conservation and electron transfer during syntrophic growth. Up-regulation of genes in a predicted operon coding for lactate uptake and oxidation suggested that the immediate fate of electrons derived from lactate oxidation differs for syntrophic and respiratory growth. Notably, this lactate dehydrogenase is homologous to a membrane-bound glycolate oxidase in *E. coli* that is directly coupled to the electron transport chain (20, 26, 34). Additionally, the *coo* genes are up-regulated and encode for a protein homologous to those found in other *Bacteria* and *Archaea* that function as proton (or sodium) translocating hydrogenases, strongly suggesting a similar electrogenic role in *Desulfovibrio* (8, 16, 22, 35). Another highly up-regulated transmembrane protein (Hmc) likely shuttles electrons from the cytoplasm to/from soluble periplasmic carriers such as cytochrome c_3 (28, 33), thus providing a possible link between cytoplasmic oxidation and periplasmic hydrogenases. There is no evidence that the Hmc has a function in direct proton translocation.

Mutants in a subset of these up-regulated genes served to confirm a direct involvement in syntrophy. The growth phenotype of the Δ*cooL* mutant is of particular significance in the proposed mechanism of syntrophic growth. This mutant affected only the lactate-grown coculture, having no affect on respiratory growth with either lactate or pyruvate, nor any significant affect on the pyruvate-grown coculture. As represented by the model presented in Figure 3 and reactions 6 and 7, electrons derived from the oxidation of lactate may be shuttled via an undefined electron carrier (EC, likely the quinone pool) to

the Coo hydrogenase. The combined reaction (reaction 8) is only favorable at very low concentrations of H_2 and pyruvate. Continuous consumption of these compounds either internally (pyruvate) or externally via the methanogen (hydrogen) contributes to a more energetically favorable condition for continued lactate oxidation. Since internal concentrations of lactate and pyruvate likely remain relatively stable, fluctuations in the hydrogen concentration primarily governs the thermodynamic feasibility of lactate oxidation. Increases in hydrogen concentration inhibit lactate oxidation by preventing the Coo hydrogenase from re-oxidizing the electron carrier. For example, at the steady-state hydrogen concentrations observed (5-6 Pa) and assuming no contribution of reverse electron flow, lactate oxidation ceases at an intracellular lactate:pyruvate ratio of approximately 1000. However, without measurements of intracellular metabolite concentrations it is not possible to constrain the requirement for reverse electron flow in the initial oxidation of lactate, as shown by the absence of free. If reverse electron flow is required for lactate oxidation, the Coo hydrogenase might provide a mechanism – if this hydrogenase uses the PMF to evolve hydrogen (rather than functioning to export protons as depicted in Figure 3).

Since a mutant in the Coo hydrogenase impairs only growth on lactate in coculture, this hydrogenase appears to be part of a dedicated system for syntrophic growth on lactate. A similar function is indicated for the Hmc, required for the reoxidation of reduced ferredoxin generated by the activity of a pyruvate-ferredoxin oxidoreductase (Por, DVU3025) (30). This activity accounts for the defective growth of this mutant in coculture on both lactate and pyruvate, with the reduced impact upon respiratory growth previously attributed to compensation by alternative transmembrane electron carriers (e.g., the Tmc and Rnf complexes) apparently specific to sulfate-reduction (6, 29, 45).

Both the Δ*hyd* and Δ*hyn-1* mutants demonstrated small differences in maximum cell density during syntrophic growth on both lactate and pyruvate, possibly because alternative periplasmic hydrogenases (Hyn-2 and Hys) masked these lesions. Their impact upon the overall coculture, but not monoculture, growth rate suggests incomplete compensation by the two alternative hydrogenases under this growth modality. The differential coculture growth rates observed likely result from the varied affinities and activities of the Hyd and Hyn-1 hydrogenases that would affect only the hydrogen production rate (27).

Some evidence suggests a role for Hdr in ethanol production and consumption (13). In association with Adh and Aor, it may reduce acetyl-CoA and produce the small quantities of ethanol produced during syntrophic growth (Figure 3, orange box). As observed in other SRM, this pathway could transiently serve as an alternative electron transport mechanism to maintain redox balance during periods of elevated hydrogen concentration (21). However, both accumulation of toxic by-products such as ethanol or acetaldehyde, and the lack of energy recovered from acetyl-CoA reduction to ethanol, make this alternative pathway unfavorable for continued growth..

Although many genes encoding electron transfer functions are up-regulated, the single mostly highly down-regulated gene in coculture codes for a flavodoxin ($\log_2 R = -5.2$). The down-regulation of this gene appears to be related to a general down-regulation of genes involved in iron and metal uptake when *D. vulgaris* is grown in coculture. This is almost certainly an indirect consequence of the absence of appreciable sulfide production by syntrophically grown *Desulfovibrio*. The formation of metal sulfides during growth by sulfate respiration greatly reduces metal availability, as reflected by the higher

expression levels in monoculture of genes for iron transport (*feoA, feoB, tonB*), molybdenum uptake (*modB*), and zinc uptake (*znuAB*; see Supplemental Table 2). A related flavodoxin in the cyanobacterium *Anabaena* replaces ferredoxin as electron carrier from photosystem I to ferredoxin-$NADP^+$ reductase under iron-deficient conditions (12). Thus, although the *Desulfovibrio* flavodoxin has been implicated as a constitutive component of the sulfate reduction pathway, its highly repressed expression in coculture suggests that it may function primarily under conditions of iron-limitation (17). Chemotaxis-related functions also comprise a general category of genes that tend to be down regulated in coculture (e.g., *cheA*, *cheY*, and multiple genes coding for methyl-accepting chemotaxis proteins [MCPs]; Supplemental Table 2), although one MCP (DVU0344) was up-regulated about 5-fold. Similar down-regulation of genes for MCPs was observed for *Rhizobium leguminosarum* following its differentiation into a plant-associated symbiotic bacteroid, suggesting that the transition from monoculture to coculture by the *Desulfovibrio* is also associated with comparable physiological change (48).

In contrast to the down-regulation of many genes for chemotaxis, several genes encoding for parts the flagellar system basal body and filament (*flgC*, *flgB*, *flgL*; Supplemental Table 2) are significantly up-regulated in coculture. Although we have no immediate explanation for these expression trends, recent studies of a similar syntrophic couple between a bacterium (*Pelotomaculum thermopropionicum*) and an archaeon (*Methanothermobacter thermautotrophicus*) have shown that the bacterial flagellum mediates physical association between the two species (38). In addition to promoting a close physical association thought to enhance syntrophy, the presence of the filament cap protein (FliD) alone induced expression of methanogen genes required for syntrophic

growth. Thus, available data are highly suggestive of specific metabolic and protein-mediated systems of communication between evolutionarily unrelated species of microorganisms.

The existence of independent electron transfer systems for syntrophic versus respiratory growth in *Desulfovibrio* also has relevance to the evolution of microorganisms functioning primarily as syntrophs. The evolutionary history of "obligate" syntrophs is closely intertwined with that of sulfate-reducers, with syntrophs appearing to have diverged on more than one occasion from sulfate-reducing ancestry. Independent energy conservation pathways functioning during sulfate-respiration and syntrophy may have permitted this evolution. The genomes of *Syntrophus aciditrophicus* (a Gram-negative deltaproteobacterium) and *Pelotomaculum themopropionicum* (related to gram-positive *Desulfotomaculum* species) tentatively support this hypothesis as both contain homologues of enzymes functioning in the syntrophic growth of *Desulfovibrio* - including Coo and Hmc, electron transfer, and ferredoxin recycling (18, 24). More importantly, *P. thermopropionicum* and several related species contain vestiges of an ancestral sulfate-reducing pathway, suggesting relatively recent adaptation to low sulfate environments (15). While environmental fluctuations of sulfate likely contributed towards evolution of an independent "syntrophic" metabolism, stable anaerobic environments lacking terminal electron acceptors may promote genomic loss of functional abilities, such as observed in the facultative syntrophs *P. thermopropionicum* and *P. schinkii*. These stable environments may assist in developing more specialized ecological niches, increasingly segregating independent energy generation pathways within divergent microbial species.

Acknowledgements

This work was part of the Virtual Institute for Microbial Stress and Survival (http://VIMSS/lbl.gov) supported by the U.S. Department of Energy, Office of Science, Office of Biological and Environmental Research, Genomics:GTL program through contract DE-AC02-05CH11231 between Lawrence Berkeley National Laboratory and the U.S. Department of Energy. *Methanococcus maripaludis* S2 strain and culturing assistance kindly provided by John Leigh (University of Washington). The authors wish to thank Professor Bernard Schink (University of Constance) and Everett Shock (Arizona State University) for thoughtful editorial assistance. Gene expression data is available at Microbes Online (www.microbesonline.org) and under GEO reference ###.

Figure 1. Representative biomass (squares), hydrogen (diamonds) and methane (crosses) profiles for a single biological coculture replicate. Continuous culture was started at hour 72 (arrow).

Figure 2. (A) Growth curves of wildtype and mutant *D. vulgaris* cocultures on lactate. Error bars represent standard deviation of triplicate cultures. (B) Maximum cell densities (as determined by $O.D._{600}$ measurements) of wildtype and mutant *D. vulgaris* cocultures and monocultures. Maximum cell densities values represent the largest $O.D._{600}$ readings observed after exponential growth. Legend symbols refer to growth curves in (A); shading refers to cell densities in (B).

Figure 3. Proposed metabolic model for syntrophic growth for *D. vulgaris* Hildenborough. Color scheme refers to transcriptional changes of individual genes during coculture growth versus sulfate-limited monoculture. EC represents an unknown electron carrier interacting with Ldh. The lactate permease is represented by DVU3026. Abbreviations: Ldh – lactate dehydrogenase (likely DVU3027), Por – pyruvate:ferredoxin oxidoreductase (DVU3025), Pta – phosphate acetyltransferase (DVU3029), Ack – acetate kinase (DVU3030), Aor – aldehyde:ferredoxin oxidoreductase (DVU1179), Adh – alcohol dehydrogenase (DVU2405), Hdr – putative heterodisulfide reductase (DVU2399 – 2404), Fd – reduced or oxidized ferredoxin, Coo – cytoplasmic hydrogenase (DVU2286-93), Hmc – high molecular weight cytochrome complex (DVU0531-6), Hyn1 – [NiFe] hydrogenase isozyme 1 (DVU1921-2), Hyd – [Fe] hydrogenase (DVU1769-70). The red box highlights unique lactate oxidation enzymes functioning during syntrophic growth. The orange box depicts the proposed hypothetical pathway of ethanol production (via hydrogen consumption).

REFERENCES

1. **Altschul, S. F., T. L. Madden, A. A. Schaffer, J. H. Zhang, Z. Zhang, W. Miller, and D. J. Lipman.** 1997. Gapped BLAST and PSI-BLAST: a new generation of protein database search programs. Nucleic Acids Res. **25:**3389-3402.
2. **Brandis, A., and R. K. Thauer.** 1981. Growth of *Desulfovibrio* species on hydrogen and sulfate as sole energy-source. J. Gen. Microbiol. **126:**249-252.
3. **Bryant, M. P., L. L. Campbell, C. A. Reddy, and M. R. Crabill.** 1977. Growth of *Desulfovibrio* in lactate or ethanol media low in sulfate in association with H2-utilizing methanogenic bacteria. Appl. Environ. Microbiol. **33:**1162-1169.
4. **Chhabra, S. R., Q. He, K. H. Huang, S. P. Gaucher, E. J. Alm, Z. He, M. Z. Hadi, T. C. Hazen, J. D. Wall, J. Zhou, A. P. Arkin, and A. K. Singh.** 2006. Global analysis of heat shock response in *Desulfovibrio vulgaris* Hildenborough. J. Bacteriol. **188:**1817-1828.
5. **Chun, K. T., H. J. Edenberg, M. R. Kelley, and M. G. Goebl.** 1997. Rapid amplification of uncharacterized transposon-tagged DNA sequences from genomic DNA. Yeast **13:**233-240.
6. **Dolla, A., B. K. J. Pohorelic, J. K. Voordouw, and G. Voordouw.** 2000. Deletion of the *hmc* operon of *Desulfovibrio vulgaris* subsp *vulgaris* Hildenborough hampers hydrogen metabolism and low-redox-potential niche establishment. Arch. Microbiol. **174:**143-151.
7. **Dudoit, S., and J. Fridlyand.** 2002. A prediction-based resampling method for estimating the number of clusters in a dataset. Genome Biol. **3:**36.
8. **Fox, J. D., R. L. Kerby, G. P. Roberts, and P. W. Ludden.** 1996. Characterization of the CO-induced, CO-tolerant hydrogenase from *Rhodospirillum rubrum* and the gene encoding the large subunit of the enzyme. J. Bacteriol. **178:**1515-1524.
9. **Fu, R. D., and G. Voordouw.** 1997. Targeted gene-replacement mutagenesis of *dcrA*, encoding an oxygen sensor of the sulfate-reducing bacterium *Desulfovibrio vulgaris* Hildenborough. Arch. Microbiol. **143:**1815-1826.
10. **Gao, H. C., Y. Wang, X. D. Liu, T. F. Yan, L. Y. Wu, E. Alm, A. Arkin, D. K. Thompson, and J. Z. Zhou.** 2004. Global transcriptome analysis of the heat shock response of *Shewanella oneidensis*. J. Bacteriol. **186:**7796-7803.
11. **Goenka, A., J. K. Voordouw, W. Lubitz, W. Gartner, and G. Voordouw.** 2005. Construction of a NiFe-hydrogenase deletion mutant of *Desulfovibrio vulgaris* Hildenborough. Biochem. Soc. Trans. **33:**59-60.
12. **Goni, G., B. Herguedas, M. Hervas, J. R. Peregrina, M. A. De la Rosa, C. Gomez-Moreno, J. A. Navarro, J. A. Hermoso, M. Martinez-Julvez, and M. Medina.** 2009. Flavodoxin: A compromise between efficiency and versatility in the electron transfer from photosystem I to ferredoxin-NADP(+) reductase. Biochim. Biophys. Acta **1787:**144-154.
13. **Haveman, S. A., V. Brunelle, J. K. Voordouw, G. Voordouw, J. F. Heidelberg, and R. Rabus.** 2003. Gene expression analysis of energy metabolism mutants of *Desulfovibrio vulgaris* Hildenborough indicates an important role for alcohol dehydrogenase. J. Bacteriol. **185:**4345-4353.
14. **Heidelberg, J. F., R. Seshadri, S. A. Haveman, C. L. Hemme, I. T. Paulsen, J. F. Kolonay, J. A. Eisen, N. Ward, B. Methe, L. M. Brinkac, S. C. Daugherty, R. T. Deboy, R. J. Dodson, A. S. Durkin, R. Madupu, W. C. Nelson, S. A. Sullivan, D. Fouts, D. H. Haft, J. Selengut, J. D. Peterson, T. M. Davidsen, N.**

Zafar, L. Zhou, D. Radune, G. Dimitrov, M. Hance, K. Tran, H. Khouri, J. Gill, T. R. Utterback, T. V. Feldblyum, J. D. Wall, G. Voordouw, and C. M. Fraser. 2004. The genome sequence of the anaerobic, sulfate-reducing bacterium *Desulfovibrio vulgaris* Hildenborough. Nat. Biotechnol. **22:**554-9.

15. **Imachi, H., Y. Sekiguchi, Y. Kamagata, A. Loy, Y. L. Qiu, P. Hugenholtz, N. Kimura, M. Wagner, A. Ohashi, and H. Harada.** 2006. Non-sulfate-reducing, syntrophic bacteria affiliated with *Desulfotomaculum* cluster I are widely distributed in methanogenic environments. Appl. Environ. Microbiol. **72:**2080-91.
16. **Kerby, R. L., S. S. Hong, S. A. Ensign, L. J. Coppoc, P. W. Ludden, and G. P. Roberts.** 1992. Genetic and physiological characterization of the *Rhodospirillum rubrum* carbon monoxide dehydrogenase system. J. Bacteriol. **174:**5284-94.
17. **Knauf, M. A., F. Lohr, M. Blumel, S. G. Mayhew, and H. Ruterjans.** 1996. NMR investigation of the solution conformation of oxidized flavodoxin from *Desulfovibrio vulgaris* - Determination of the tertiary structure and detection of protein-bound water molecules. Eur. J. Biochem. **238:**423-434.
18. **Kosaka, T., S. Kato, T. Shimoyama, S. Ishii, T. Abe, and K. Watanabe.** 2008. The genome of *Pelotomaculum thermopropionicum* reveals niche-associated evolution in anaerobic microbiota. Genome Res. **18:**442-8.
19. **Larsen, R. A., M. M. Wilson, A. M. Guss, and W. W. Metcalf.** 2002. Genetic analysis of pigment biosynthesis in *Xanthobacter autotrophicus* Py2 using a new, highly efficient transposon mutagenesis system that is functional in a wide variety of bacteria. Arch. Microbiol. **178:**193-201.
20. **Lord, J. M.** 1972. Glycolate oxidoreductase in *Escherichia coli*. Biochim. Biophys. Acta **267:**227-37.
21. **Ma, K., and M. W. Adams.** 1999. An unusual oxygen-sensitive, iron- and zinc-containing alcohol dehydrogenase from the hyperthermophilic archaeon *Pyrococcus furiosus*. J. Bacteriol. **181:**1163-70.
22. **Maness, P. C., J. Huang, S. Smolinski, V. Tek, and G. Vanzin.** 2005. Energy generation from the CO oxidation-hydrogen production pathway in *Rubrivivax gelatinosus*. Appl. Environ. Microbiol. **71:**2870-2874.
23. **McInerney, M. J., and M. P. Bryant.** 1981. Anaerobic Degradation of lactate by syntrophic associations of *Methanosarcina barkeri* and *Desulfovibrio* species and effect of H2 on acetate degradation. Appl. Environ. Microbiol. **41:**346-354.
24. **McInerney, M. J., L. Rohlin, H. Mouttaki, U. Kim, R. S. Krupp, L. Rios-Hernandez, J. Sieber, C. G. Struchtemeyer, A. Bhattacharyya, J. W. Campbell, and R. P. Gunsalus.** 2007. The genome of *Syntrophus aciditrophicus*: life at the thermodynamic limit of microbial growth. Proc. Natl. Acad. Sci. U.S.A. **104:**7600-5.
25. **Mukhopadhyay, A., Z. L. He, E. J. Alm, A. P. Arkin, E. E. Baidoo, S. C. Borglin, W. Q. Chen, T. C. Hazen, Q. He, H. Y. Holman, K. Huang, R. Huang, D. C. Joyner, N. Katz, M. Keller, P. Oeller, A. Redding, J. Sun, J. Wall, J. Wei, Z. M. Yang, H. C. Yen, J. Z. Zhou, and J. D. Keasling.** 2006. Salt stress in *Desulfovibrio vulgaris* Hildenborough: An integrated genomics a pproach. J. Bacteriol. **188:**4068-4078.
26. **Ornston, L. N., and M. K. Ornston.** 1969. Regulation of glyoxylate metabolism in *Escherichia coli* K-12. J. Bacteriol. **98:**1098-108.
27. **Peck, H. D., Jr.** 1994. Molecular Biology of the Sulfate-Reducing Bacteria, p. 41-75. *In* J. M. Odom and J. Singleton, R. (ed.), The Sulfate-Reducing Bacteria: Contemporary Perspectives. Springer Verlag, New York.

28. **Pereira, I. A. C., C. V. Romao, A. V. Xavier, J. LeGall, and M. Teixeira.** 1998. Electron transfer between hydrogenases and mono- and multiheme cytochromes in *Desulfovibrio* ssp. J. Biol. Inorg. Chem. **3:**494-498.
29. **Pereira, P. M., M. Teixeira, A. V. Xavier, R. O. Louro, and I. A. C. Pereira.** 2006. The Tmc complex from *Desulfovibrio vulgaris* Hildenborough is involved in transmembrane electron transfer from periplasmic hydrogen oxidation. Biochemistry **45:**10359-10367.
30. **Pieulle, L., B. Guigliarelli, M. Asso, F. Dole, A. Bernadac, and E. C. Hatchikian.** 1995. Isolation and characterization of the pyruvate-ferredoxin oxidoreductase from the sulfate-reducing bacterium *Desulfovibrio africanus*. Biochim. Biophys. Acta **1250:**49-59.
31. **Pohorelic, B. K. J., J. K. Voordouw, E. Lojou, A. Dolla, J. Harder, and G. Voordouw.** 2002. Effects of deletion of genes encoding Fe-only hydrogenase of *Desulfovibrio vulgaris* Hildenborough on hydrogen and lactate metabolism. J. Bacteriol. **184:**679-686.
32. **Rabus, R., T. Hansen, and F. Widdle.** 2006. Dissimilatory Sulfate- and Sulfur-Reducing Prokaryotes. *In* M. Dworkin, S. Falkow, E. Rosenberg, K. H. Schleifer, and E. Stackebrandt (ed.), The Prokaryotes: An Evolving Electronic Resource for the Microbiological Community, 3rd edition, release 3.3 ed. Springer-Verlag, New York.
33. **Rossi, M., W. B. R. Pollock, M. W. Reij, R. G. Keon, R. D. Fu, and G. Voordouw.** 1993. The *hmc* operon of *Desulfovibrio vulgaris* subsp *vulgaris* Hildenborough encodes a potential transmembrane redox protein complex. J. Bacteriol. **175:**4699-4711.
34. **Sallal, A. K., and N. A. Nimer.** 1989. The intracellular localization of glycolate oxidoreductase in *Escherichia coli*. FEBS Lett. **258:**277-80.
35. **Sapra, R., M. Verhagen, and M. W. W. Adams.** 2000. Purification and characterization of a membrane-bound hydrogenase from the hyperthermophilic archaeon *Pyrococcus furiosus*. J. Bacteriol. **182:**3423-3428.
36. **Schink, B.** 1997. Energetics of syntrophic cooperation in methanogenic degradation. Microbiol. Mol. Biol. Rev. **61:**262-280.
37. **Schink, B.** 2002. Synergistic interactions in the microbial world. Antonie van Leeuwenhoek **81:**257-61.
38. **Shimoyama, T., S. Kato, S. Ishii, and K. Watanabe.** 2009. Flagellum mediates symbiosis. Science **323:**1574-1574.
39. **Stams, A. J. M., C. M. Plugge, F. A. M. de Bok, B. van Houten, P. Lens, H. Dijkman, and J. Weijma.** 2005. Metabolic interactions in methanogenic and sulfate-reducing bioreactors. Water Sci. Technol. **52:**13-20.
40. **Stolyar, S., S. Van Dien, K. L. Hillesland, N. Pinel, T. J. Lie, J. A. Leigh, and D. A. Stahl.** 2007. Metabolic modeling of a mutualistic microbial community. Mol. Syst. Biol. **3:**92.
41. **Talaat, A. M., S. T. Howard, W. Hale IV, R. Lyons, H. Garner, and S. A. Johnston.** 2002. Genomic DNA standards for gene expression profiling in *Mycobacterium tuberculosis*. Nucleic Acids Res. **30:**e104.
42. **Thauer, R. K., K. Jungermann, and K. Decker.** 1977. Energy conservation in chemotrophic anaerobic bacteria. Bacteriol. Rev. **41:**100-80.
43. **Thompson, D. K., A. S. Beliaev, C. S. Giometti, S. L. Tollaksen, T. Khare, D. P. Lies, K. H. Nealson, J. Lim, J. Yates, C. C. Brandt, J. M. Tiedje, and J. Z. Zhou.** 2002. Transcriptional and proteomic analysis of a ferric uptake regulator (Fur) mutant of *Shewanella oneidensis*: possible involvement of Fur in energy

metabolism, transcriptional regulation, and oxidative stress. Appl. Environ. Microbiol. **68:**881-892.

44. **Traore, A. S., M. L. Fardeau, C. E. Hatchikian, J. Legall, and J. P. Belaich.** 1983. Energetics of growth of a defined mixed culture of *Desulfovibrio vulgaris* and *Methanosarcina barkeri* - Interspecies hydrogen transfer in batch and continuous cultures. Appl. Environ. Microbiol. **46:**1152-1156.

45. **Voordouw, G.** 2002. Carbon monoxide cycling by *Desulfovibrio vulgaris* Hildenborough. J. Bacteriol. **184:**5903-5911.

46. **Widdel, F., and F. Bak.** 1992. Gram-negative sulfate-reducing bacteria, p. 3352-3378. *In* A. Ballows, H. G. Trueper, M. Dworkin, W. Harder, and K. H. Schleifer (ed.), The Prokaryotes: A Handbook on the Biology Bacteria: Ecophysiology, Isolation, Identification, Application, 2rd edition ed. Springer-Verlag, New York.

47. **Williams, B. A., R. M. Gwirtz, and B. J. Wold.** 2004. Genomic DNA as a cohybridization standard for mammalian microarray measurements. Nucleic Acids Res. **32:**e81.

48. **Yost, C. K., K. L. Del Bel, J. Quandt, and M. F. Hynes.** 2004. *Rhizobium leguminosarum* methyl-accepting chemotaxis protein genes are down-regulated in the pea nodule. Arch. Microbiol. **182:**505-513.

49. **Zhang, W. W., D. E. Culley, J. C. M. Scholten, M. Hogan, L. Vitiritti, and F. J. Brockman.** 2006. Global transcriptomic analysis of *Desulfovibrio vulgaris* on different electron donors. Antonie van Leeuwenhoek Int. J. of Gen. and Mol. Microbiol. **89:**221-237.

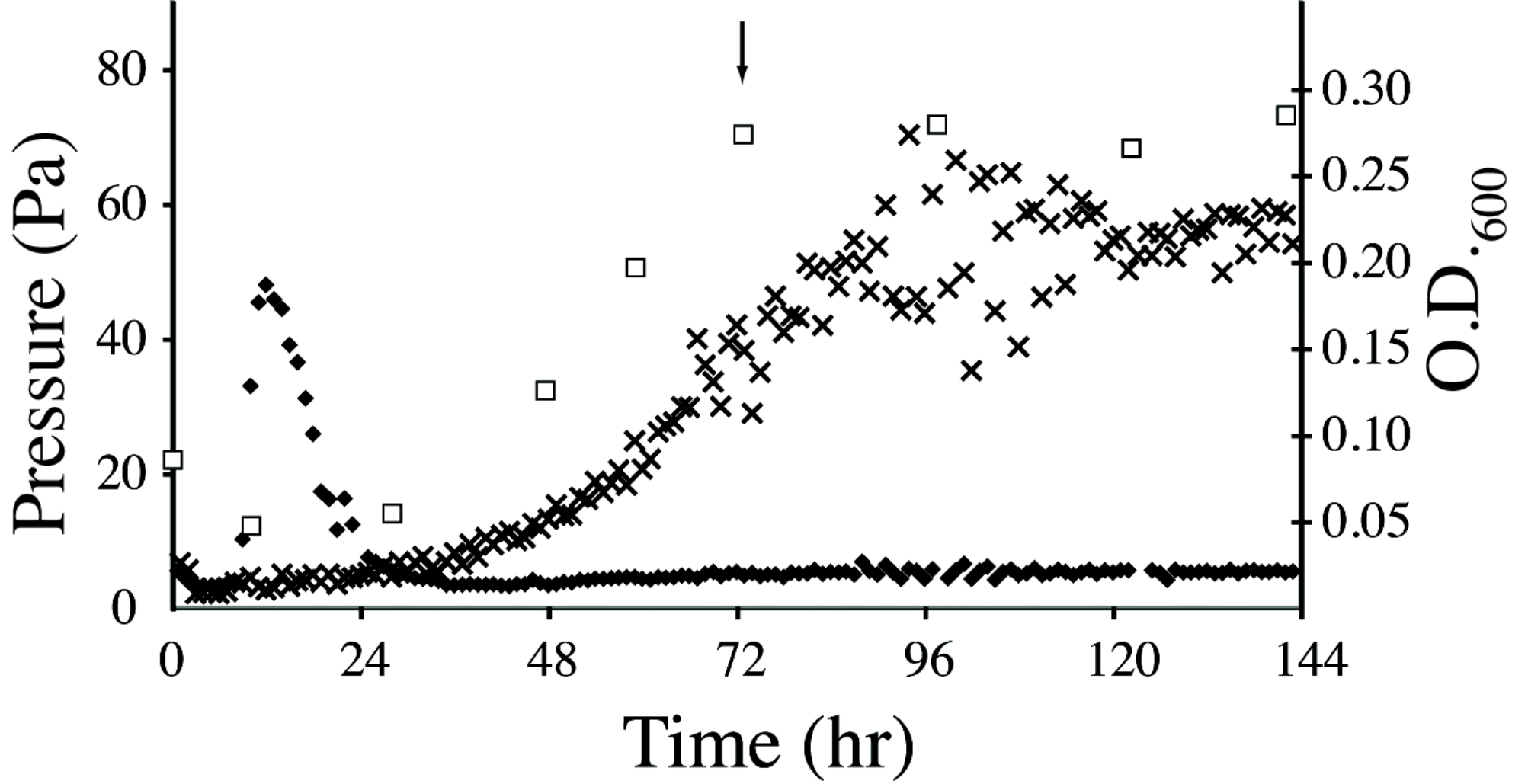
Pressure (Pa)
0
20
40
60
80
O.D.600
0.05
0.10
0.15
0.20
0.25
0.30
0
24
48
72
96
120
144
Time (hr)

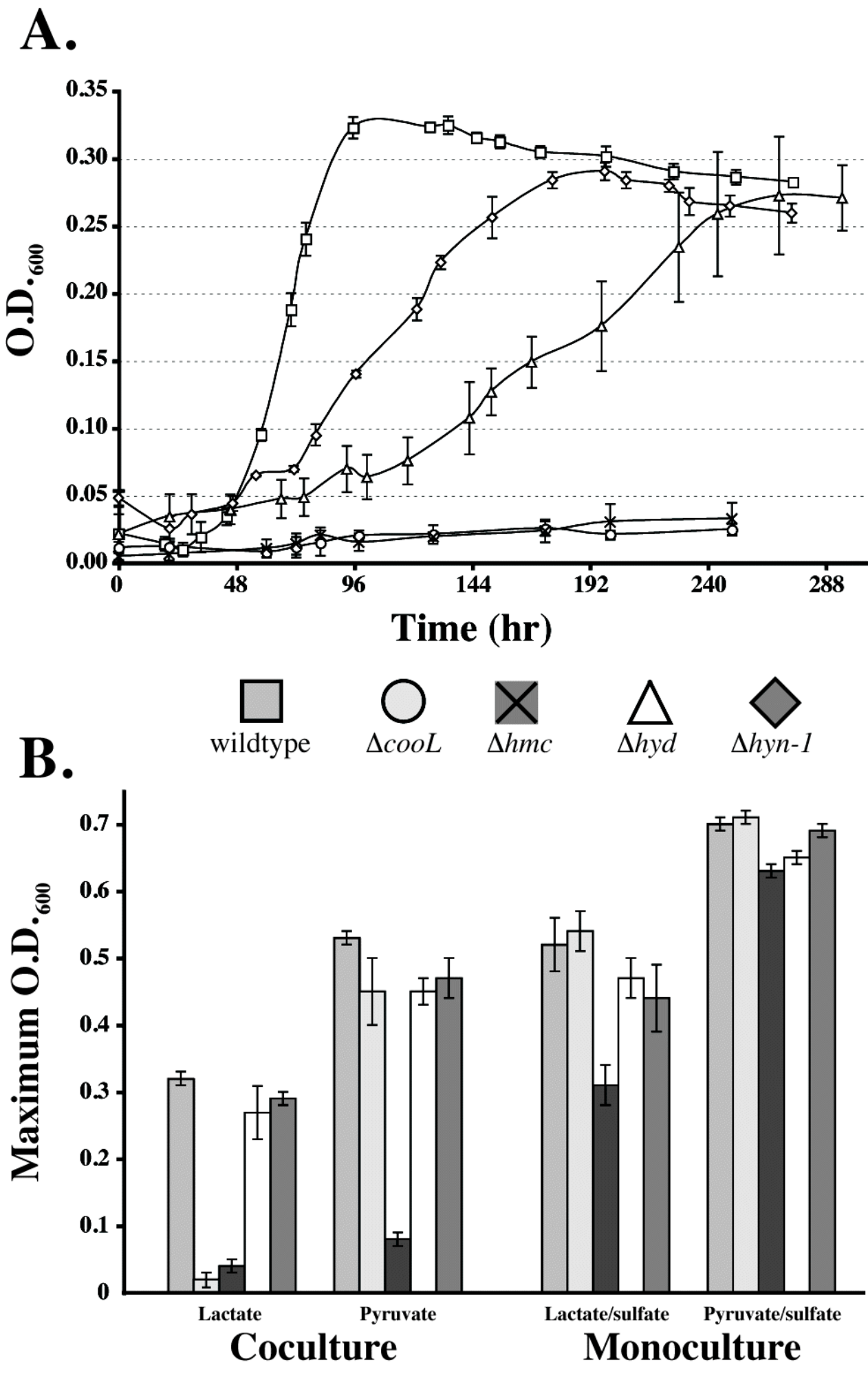
A.
O.D.600
0.35
0.30
0.25
0.20
0.15
0.10
0.05
0.00
0
48
96
144
192
240
288
Time (hr)
wildtype
ΔcooL
Δhmc
Δhyd
Δhyn-1
B.
Maximum O.D.600
0.7
0.6
0.5
0.4
0.3
0.2
0.1
0
Lactate
Pyruvate
Lactate/sulfate
Pyruvate/sulfate
Coculture
Monoculture

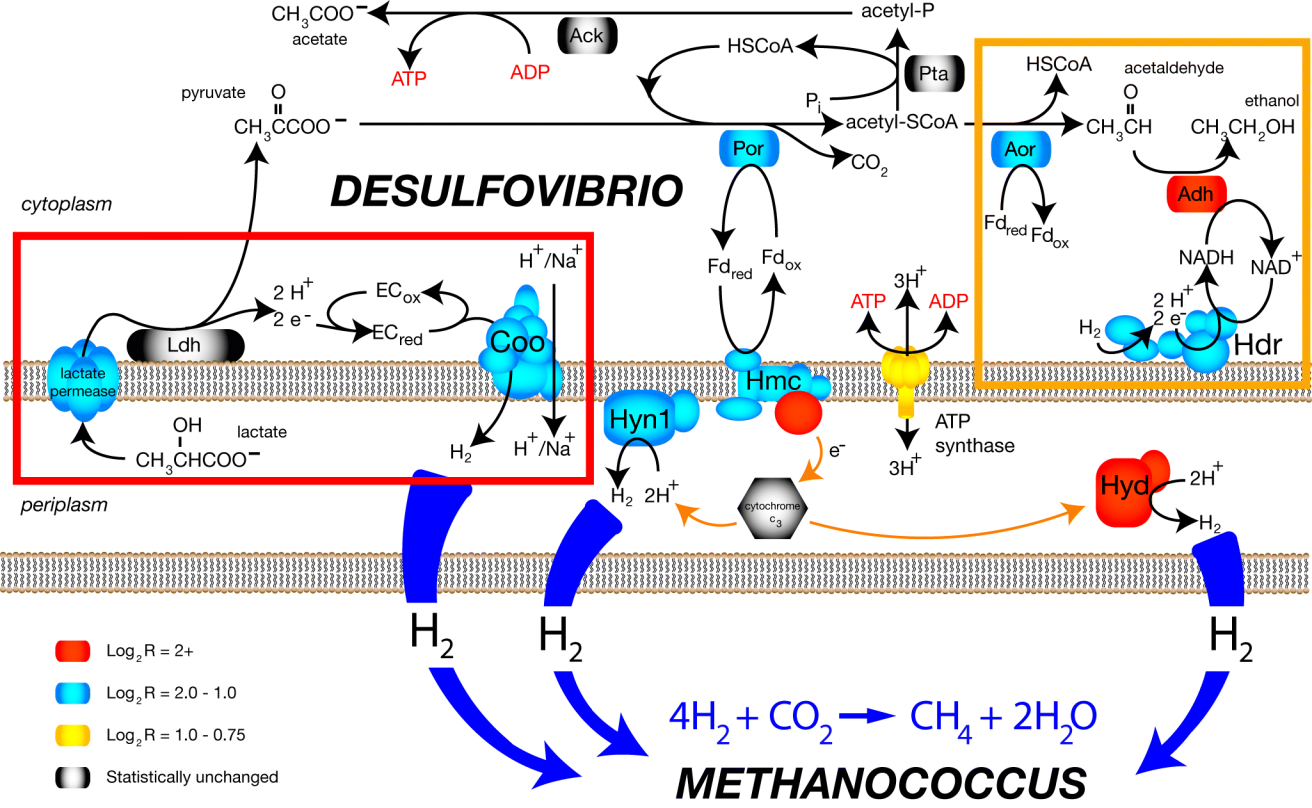
CH3COO−
acetate
ATP
ADP
Ack
acetyl-P
HSCoA
Pta
Pi
acetyl-SCoA
CO2
pyruvate
CH3CCOO−
Por
DESULFOVIBRIO
cytoplasm
periplasm
Fdred
Fdox
3H+
ATP
ADP
ATP synthase
3H+
HSCoA
acetaldehyde
CH3CH
ethanol
CH3CH2OH
Aor
Fdred
Fdox
Adh
NADH
NAD+
2 H+
2 e−
H2
Hdr
H+/Na+
2 H+
2 e−
ECox
ECred
Ldh
Coo
lactate permease
OH
lactate
CH3CHCOO−
H+/Na+
Hmc
Hyn1
H2
2H+
e−
cytochrome c3
Hyd
2H+
H2
H2
H2
H2
Log2R = 2+
Log2R = 2.0 - 1.0
Log2R = 1.0 - 0.75
Statistically unchanged
4H2 + CO2 → CH4 + 2H2O
METHANOCOCCUS

Table 1: Strains used during this investigation.

Strain	Mutant	Gene(s)	Description	Source
Desulfovibrio vulgaris Hildenborough (ATCC 29579)	*n.a.*	*n.a.*	Wildtype strain	ATCC
JW3040	Δ*cooL*	DVU2288	Transposon-interruption of 3rd gene in CO-induced hydrogenase	This study
H801	Δ*hmc*	DVU0532-5	Deletion mutant of hmcBCDE	Dolla *et al*., 2000
Hyd100	Δ*hyd*	DVU1679-70	Deletion mutant of hydAB	Pohorelic *et al*., 2002
NiFe100	Δ*hyn*	DVU1921-2	Deletion mutant of hynAB-1	Goenka *et al*., 2004
Methanococcus maripaludis S2	*n.a.*	*n.a.*	Wildtype strain	Whitman *et al*., 1986

Table 2: Estimated growth yields (g dry cell biomass/mol substrate) of wildtype cocultures and monocultures grown on lactate or pyruvate (30 mM). Monocultures were grown with 30 mM sulfate. Coculture from Traore *et al*., contained *D. vulgaris* and *Methanosarcina barkeri*. All lactate:pyruvate, $lactate_{coculture}$:$lactate_{monoculture}$ and $pyruvate_{coculture}$:$pyruvate_{monculture}$ ratios calculated based on growth yields listed here. Error represents the standard deviation of triplicate samples.

Strain	***COCULTURE***			***MONOCULTURE***			$Lactate_{CO}$:$Lactate_{MONO}$	$Pyruvate_{CO}$:$Pyruvate_{MONO}$
	Lactate	Pyruvate	Lactate:Pyruvate	Lactate	Pyruvate	Lactate:Pyruvate		
wildtype	4.2 ± 0.1	6.8 ± 0.3	0.61 ± 0.05	5.0 ± 0.4	7.2 ± 0.1	0.69 ± 0.08	0.83 ± 0.08	0.94 ± 0.05
Traore *et al*., 1983	5.3 ± 0.9	6.3 ± 0.9	0.84 ± 0.22	6.7 ± 1.2	10.1 ± 1.7	0.66 ± 0.25	0.79 ± 0.25	0.62 ± 0.22